Arch. Mech., **65**, 4, pp. 265–288, Warszawa 2013

Continuous model for flexural vibration analysis of a Timoshenko cracked beam

M. HEYDARI, A. EBRAHIMI, M. BEHZAD

Sharif University of Technology
Mechanical Engineering Department
P.O. Box 11365-9567, Azadi Ave.
Tehran, Iran
e-mail: mheydari1985@gmail.com

In this paper, a continuous model for vibration analysis of a beam with an open edge crack including the effects of shear deformation and rotary inertia is presented. A displacement field is suggested for the beam and the strain, and stress fields are calculated. The governing equation of motion for the beam has been obtained using Hamilton's principle. The equation of motion is solved with a modified Galerkin method and the natural frequencies and mode shapes are obtained. A good agreement has been observed between the results of this research and the results of previous work done in this fiels. The results are also compared to results of a similar model with Euler-Bernoulli assumptions to confirm the advantages of the proposed model in the case of short beams.

Key words: vibration analysis, cracked beam, Timoshenko beam, Galerkin's method, continuous model.

1. Introduction

Structural defects such as cracks may be produced in structures and machineries under fatigue load operating conditions. The presence of crack can lead to catastrophic failures in certain conditions. Therefore, developing methods for early detection of cracks has been the subject of many researches. One of these methods is the vibration analysis of cracked structures. The occurrence of cracks affects the dynamic and vibration behavior of the structure considerably. These vibrations can be used for identifying the cracks and thereby appropriate actions can be taken to prevent more damage to the system.

The vibration behavior of cracked structures has been investigated by many researchers. Dimarogonas [1] presented a review on the topic of vibration of cracked structures. His review included the vibration analysis of cracked rotors, bars, beams, plates, pipes, blades and shells. Two more literature reviews by Wauer and Gasch [2, 3] on the dynamic behavior of cracked rotors – are also available.

Beams are important elements in structures and machineries; thus, the vibration behavior of cracked beams has been extensively studied by researchers. There exist three methods for the vibration modeling of cracked beams: discrete models with a local flexibility model for the crack, continuous models with a local flexibility model for the crack, and continuous models with a continues model for the crack. Dimarogonas [4] was the first who suggested the local flexibility method for modeling the crack. He replaced the crack by a rotational spring connecting two healthy half-beams. The stiffness of this spring was obtained from the concept of J-integral in fracture mechanics. This local flexibility idea has been followed by several researchers till now. Some researchers utilized the first approach and modeled two healthy half-beams discretely and added the flexibility of the rotational spring to the flexibility matrix of the system [5, 6]. While others used the second approach and modeled two healthy half-beams continuously and used appropriate boundary conditions for each part to link them through the rotational spring [7, 8]. Loya *et al.* [9] developed a local flexibility model for the flexural vibrations of Timoshenko cracked beams. They also modified the local flexibility model of the crack by adding one or two linear springs beside the rotational one. These methods have also been extended for beams with more than one crack [10–12].

The local flexibility model for the crack is a simple approach and has a relatively good result in finding fundamental natural frequency of a cracked beam. However, this method offers no solutions for finding the stress at the crack area under the dynamic loads, mode shapes in free vibrations and operational deformed shape in forced vibrations. The third approach, continuous modeling of the crack, was first developed by Christides and Barr [13]. Christides and Barr proposed a continuous theory for vibration analysis of a uniform Euler–Bernoulli beam containing one or more pairs of symmetric cracks. They suggested some modifications on the familiar stress field of a normal Euler–Bernoulli beam in order to consider the crack effect. The differential equation of motion and corresponding boundary conditions were obtained as the results. However, in their model, two different and incompatible assumptions have been made for displacement and strain fields. Although the accuracy of the results in finding the natural frequencies is acceptable for some applications, their model is not fully reliable for more accurate analyses such as stress analysis near the crack tip under dynamic loading and mode shape analysis. In addition, the resulting partial differential equation is complicated and it is dependent on some constants which are unknown and must be calculated by correlating the analytically obtained results with those calculated by the finite element method in each case. Several researchers followed the Christides and Barr's approach by modifying their method and achieved some improvements [14–18]. However, there still exists the inconsistency between strain and displacement fields which causes inaccuracy in results, especially in mode shapes and stress analysis. CARNEIRO and INMAN [19] extended Christides and Barr's approach to the case of Timoshenko cracked beams.

BEHZAD *et al.* [20] presented a new continuous theory for bending analysis of a cracked beam. A bilinear displacement field has been suggested for the beam strain and stress calculations and the bending differential equation has been obtained using the equilibrium equations. The model can predict the load-deflection relation of the beam near or far from the crack tip accurately and can be also used for stress-strain analysis in a cracked beam. This model is also used for vibration analysis of a cracked beam and excellent performance in dynamic loading has been observed [21, 22]. This method has been used for the force vibration analysis of beams with a horizontal edge crack [23]. They also extended their model to a continuous model for a beam with an edge crack perpendicular to the neutral plane (vertical edge crack) [24].

The effects of shear deformation and rotary inertia are not negligible in the case of short (Timoshenko) beams. Therefore, in this research the formulation of Behzad's model [21] is extended to the case of Timoshenko cracked beam model. The results of this study are compared with the finite element and CARNEIRO and INMAN'S [19] results for verification. In addition, the results are compared with Euler–Bernoulli model [21] to confirm the advantages of the presented model in the case of short beams.

2. Displacement field

In this research, the beam is assumed to be a prismatic beam and the crack is considered as an open edge U-shape notch. The plane strain assumption has been used and consequently the displacements along y-axis have been neglected. The displacements and stresses are supposed to be small and the crack does not become larger. Finally, the material is assumed to be linear elastic.

In this paper, a similar displacement field to Behzad's model [21] is proposed. The horizontal line passing through the crack tip is called "deviation line" which is shown in Fig. 1. It is proposed that under pure moment each straight plane section turns into two planes with different slopes, one beneath and the other above the deviation line as shown in Fig. 1. The slope difference between these two planes decreases while the distance from the crack increases. So, the following displacement field can be assumed for a cracked beam [21]:

$$\text{(2.1)} \qquad \begin{cases} w = w(x,t), & \text{(a)} \\ v = 0, & \text{(b)} \\ u(x,z,t) = u_0(x,t) - z\psi(x,t) + \Delta(x,z,t)h(z). & \text{(c)} \end{cases}$$

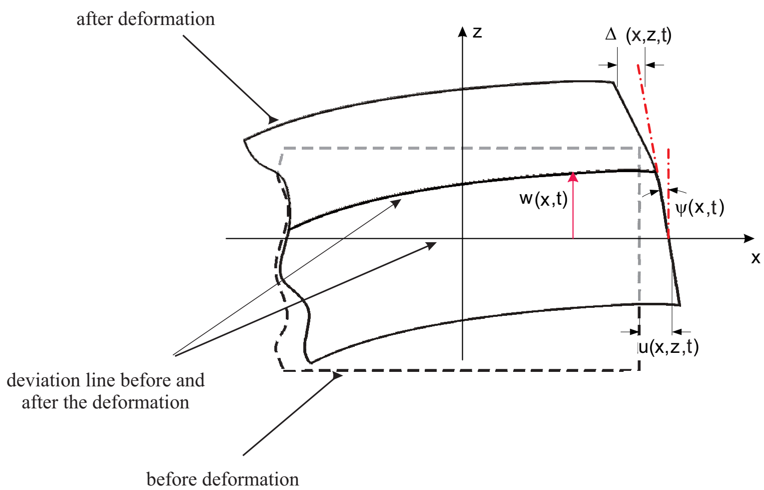

Fig. 1. Displacement field parameters of a cracked beam.

In which u, v and w are the displacement components along x, y and z axes. $u_0(x,t)$ is the longitudinal displacement of the deviation line along the x-axis and $\psi(x,t)$is the slope of plane sections below the deviation line. $h(z)$ is the unit step function which is equal to zero for $z \leq 0$ and 1 for $z > 0$. The term $\Delta(x,z)h(z)$ can be considered as the extra displacement of plane sections above the deviation line. Figure 1 shows these parameters graphically.

It is assumed that the additional displacement of the plane section above the deviation line has its maximum value at the crack faces and decreases exponentially with distance from the crack tip. Therefore, $\Delta(x,z,t)$ reads as follows:

$$\Delta(x,z,t) = \varphi(z,t)e^{-\alpha|x-x_c|/d}\,\mathrm{sgn}(x-x_c). \tag{2.2}$$

In Eq. (2.2), $\varphi(z,t)$ is the magnitude of the additional displacement at the crack faces, α is a dimensionless exponential decay rate which will be discussed later in this paper, x_c is the crack position, $d$is the depth of the beam and $\mathrm{sgn}(x-x_c)$ is the sign function. The application of the sign function is due to the fact that the additional displacement function has a discontinuity at the position of the crack and the sign of its value changes when passing through the crack tip.

In order to find $\varphi(z,t)$, a zero normal stress condition at the crack faces can be used. Thus, the normal strain function can be found using Eq. (2.2) as

$$\varepsilon_x = u_{,x} = u_{0,x} - z\psi_{,x} - \frac{\alpha}{d}\varphi(z,t)e^{-\alpha|x-x_c|/d}h(z), \tag{2.3}$$

in which the subscript $,x$ denotes the partial derivative with respect to x. The normal stress at the crack faces, $x = x_c^+$ or x_c^- and $z > 0$, should be zero.

Therefore, one has

$$\varphi(z,t) = \frac{d}{\alpha}\left(u_{0,x}(x_c,t) - z\psi_{,x}(x_c,t)\right). \tag{2.4}$$

To avoid discontinuity at the crack tip and considering the nonlinearity at the crack tip, the function $\varphi(z,t)$ can be modified as follows:

$$\varphi(z,t) = \frac{d}{\alpha}(u_{0,x}(x_c,t)(1-e^{-\beta z/d}) - z\psi_{,x}(x_c,t)), \tag{2.5}$$

where β is a dimensionless parameter and will be discussed later in this paper. The term $(1-e^{-\beta z/d})$ prevents the discontinuity at the crack tip.

3. Equation of motion

Now the strain field can be extracted from the displacement field by direct derivation. The only nonzero components of the stress field ε_x and γ_{xy} are as follows:

$$\begin{cases} \varepsilon_x = u_{,x} \\ \quad = u_{0,x} - z\psi_{,x} \\ \qquad - \left(u_{0,x}(x_c,t) - u_{0,x}(x_c,t)e^{-\beta z/d} - z\psi_{,x}(x_c,t)\right) h(z) e^{-\alpha|x-x_c|/d}, \\ \gamma_{xy} = \frac{1}{2}(w_{,x} + u_{,z}) \\ \quad = \frac{1}{2}\Bigg(w_{,x} - \psi + \left(\frac{\beta}{\alpha}u_{0,x}(x_c,t)e^{-\beta z/d} - \frac{d}{\alpha}\psi_{,x}(x_c,t)\right) \\ \qquad \times e^{-\alpha|x-x_c|/d}\,\mathrm{sgn}(x-x_c)h(z)\Bigg). \end{cases} \tag{3.1}$$

The normal and shear stress energies of the Timoshenko beam can be obtained using the following relations:

$$V_1 = \frac{1}{2}\int_V \sigma_{xx}\varepsilon_{xx} d\mathrm{V} = \frac{1}{2}\mathrm{E}\int_V \varepsilon_{xx}^2 d\mathrm{V}, \tag{3.2}$$

$$V_2 = \frac{1}{2}\int_V G\kappa\gamma_{xy}^2 d\mathrm{V}, \tag{3.3}$$

in which V_1 and V_2 are the normal and shear strain energy functions respectively, V is the volume of the beam, E is the modulus of elasticity, G is the shear modulus of elasticity and κ is the Timoshenko shear coefficient. The total potential energy can be calculated by adding up the normal and shear strain energies:

$$V_t = V_1 + V_2. \tag{3.4}$$

The total kinetic energy of the cracked beam can be also calculated as follows:

$$T_t = T_1 + T_2, \tag{3.5}$$

where T_1 and T_2, the kinetic energies due to the vertical displacement and the rotary inertia respectively, can be calculated as

$$T_1 = \frac{1}{2}\int_{\mathrm{V}} \rho w_{,t}^2 d\mathrm{V}, \tag{3.6}$$

$$T_2 = \frac{1}{2}\int_{\mathrm{V}} \rho z_\eta^2 \psi_{,t}^{*2 d}\mathrm{V}, \tag{3.7}$$

in which the rotation ψ^* can be calculated as

$$\begin{aligned}\psi^*(x,z,t) &= -\frac{u(x,z,t)-u_0(x,t)}{z}\\ &= \psi(x,t) + \frac{d}{\alpha}\psi_{,x}(x_c,t)h(z)e^{-\alpha|x-x_c|/d}\operatorname{sgn}(x-x_c)\end{aligned} \tag{3.8}$$

and z_η is position relative to the centroid in the z direction. In the other words, it is the distance from the horizontal axis η passing through the centroid of the cross-section shown in Fig. 2.

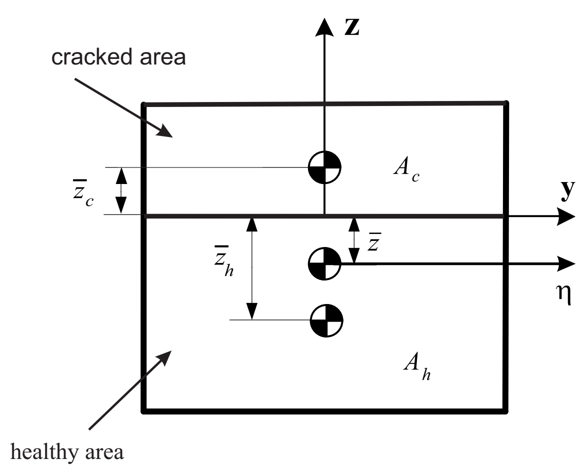

Fig. 2. Cracked beam parameter definition.

Using Hamilton's principle, one obtains

$$\delta\int_{t_0}^{t_1} L dt = \delta\int_{t_0}^{t_1}(T_t - V_t)dt = 0. \tag{3.9}$$

Now, by substituting Eq. (3.1) into Eq. (3.8) in Eq. (3.9) and performing appropriate calculations the following equations can be obtained:

$$
(3.10)\qquad \begin{cases} (\psi_{,x} - k_5\psi_{,x}(x_c,t)e^{-\alpha|x-x_c|/d})_{,xx} + \dfrac{\rho A}{EI_\eta}w_{,tt}, \\ \qquad = \dfrac{\rho}{E}(\psi_x - k_4\psi_{,x}(x_c,t)e^{-\alpha|x-x_c|/d})_{,tt}, & \text{(a)} \\ \kappa(w_{,xx} - \psi_{,x} + k_6\psi_{,x}(x_c,t)e^{-\alpha|x-x_c|/d}) = \dfrac{\rho}{G}w_{,tt}, & \text{(b)} \end{cases}
$$

where the parameters k_{1-6} are geometrical dimensionless constants which can be defined as follows:

$$
(3.11)\qquad \begin{cases} k_1 = \dfrac{1}{A_c}\displaystyle\int\limits_{A_c} e^{-\beta z/d}dA, \\ k_2 = \dfrac{A_h}{A_h + k_1A_c}, \\ k_3 = \dfrac{A_c}{A}\left(k_2 - k_1k_2 - \dfrac{\bar{z}_c}{\bar{z}_h}\right), \\ k_4 = \dfrac{I_{c_\eta}}{I_\eta}, \\ k_5 = \dfrac{(k_1-1)A_c\bar{z}_c\,(\bar{z} + k_3\bar{z}_h) + I_{c_\eta}}{I_\eta}, \\ k_6 = \dfrac{A_c}{A}\left(1 + \dfrac{\beta}{d}(\bar{z} + k_3\bar{z}_h)k_1\right), \end{cases}
$$

in which $\bar{z}$ is the vertical coordinate of the centroid of the cross-section and $\bar{z}_h$ is the vertical coordinate of the centroid of the healthy part of the cross-section as shown in Fig. 2, A is the cross-section area of the beam, A_c is the crack face area, I_{cy} is the moment of inertia of the crack face about the y-axis and I_η is the moment of inertia of the cross-section about the horizontal axis η.

By evaluating Eq. (3.10b) at the crack position, i.e., $x = x_c$, $\psi_{,x}(x_c,t)$ can be obtained as

$$
(3.12)\qquad \psi_{,x}(x_c,t) = \frac{1}{1-k_6}\left(w_{,xx}(x_c,t) - \frac{\rho}{\kappa G}w_{,tt}(x_c,t)\right).
$$

Substituting Eq. (3.12) into Eq. (3.10b), one obtains

$$
(3.13)\qquad \begin{aligned} \psi_{,x} = {} & \left(w_{,xx} - \frac{\rho}{\kappa G}w_{,tt}\right) \\ & + \frac{k_6}{1-k_6}\left(w_{,xx}(x_c,t) - \frac{\rho}{\kappa G}w_{,tt}(x_c,t)\right)e^{-\alpha|x-x_c|/d}. \end{aligned}
$$

Substituting Eqs. (3.12) and (3.13) into Eq. (3.10a), the equation of motion for free vibrations of a cracked Timoshenko beam reads as follows:

$$\left(w_{,xx}-\frac{\rho}{\kappa G}w_{,tt}+k_7\left(w_{,xx}-\frac{\rho}{\kappa G}w_{,tt}\right)(x_c,t)e^{-\alpha|x-x_c|/d}\right)_{,xx}+\frac{\rho A}{EI_\eta}w_{,tt} = \frac{\rho}{E}\left(w_{,xx}-\frac{\rho}{\kappa G}w_{,tt}+k_8\left(w_{,xx}-\frac{\rho}{\kappa G}w_{,tt}\right)(x_c,t)e^{-\alpha|x-x_c|/d}\right)_{,tt} \tag{3.14}$$

in which the parameters k_7 and k_8 can be defined as follows:

$$k_7=\frac{k_6-k_5}{1-k_6},\qquad k_8=\frac{k_6-k_4}{1-k_6}. \tag{3.15}$$

4. Calculation of exponential decay rates α and β

The dimensionless exponential decay rates (α,β) are the only factors which has not been discussed yet. In this section the parameters α and β are calculated. It has been shown that the exponential decay rate β has a very large value and accordingly it can be assumed that the parameter β tends to infinity ($\beta\to\infty$) without losing the accuracy of the results [20, 21]. Then, the parameters k_4, k_5 and k_6 in Eq. (3.11) can be simplified as follows:

$$\begin{cases} k_4=\dfrac{I_{c\eta}}{I_\eta}, \\ k_5=k_4-\dfrac{A_c\bar{z}_c}{I_\eta}\left(\bar{z}+\dfrac{A_c}{A}(\bar{z}_h-\bar{z}_c)\right), \\ k_6=\dfrac{A_c}{A}. \end{cases} \tag{4.1}$$

Using the J-integral and remote point rotation concepts, BEHZAD *et al.* [20] have shown that the exponential decay rate α can be calculated by solving the following equation:

$$\frac{\chi}{1+\chi}(e^{-\alpha x_c/d}+e^{-\alpha(l-x_c)/d}-2)-6\pi(1-\nu^2)\varphi\left(\frac{a}{d}\right)\alpha=0, \tag{4.2}$$

where χ can be calculated as follows

$$\lim_{\beta\to\infty}\chi=\left(\frac{a}{d}\right)\left(\frac{a}{d}-2\right) \tag{4.3}$$

and $\varphi\left(\frac{a}{d}\right)$ is a function of the crack depth ratio (a/d) and defined as

$$\varphi\left(\frac{a}{d}\right) = 21.8\left(\frac{a}{d}\right)^{10} - 45.8\left(\frac{a}{d}\right)^{9} + 53.8\left(\frac{a}{d}\right)^{8} - 38.5\left(\frac{a}{d}\right)^{7} + 24.4\left(\frac{a}{d}\right)^{6} - 12.5\left(\frac{a}{d}\right)^{5} + 6.14\left(\frac{a}{d}\right)^{4} - 1.57\left(\frac{a}{d}\right)^{3} + 1.26\left(\frac{a}{d}\right)^{2}. \tag{4.4}$$

α values versus the crack depth ratio $\left(\frac{a}{d}\right)$ for crack position at the midspan $(x_c = 0.5)$ are presented in Fig. 3.

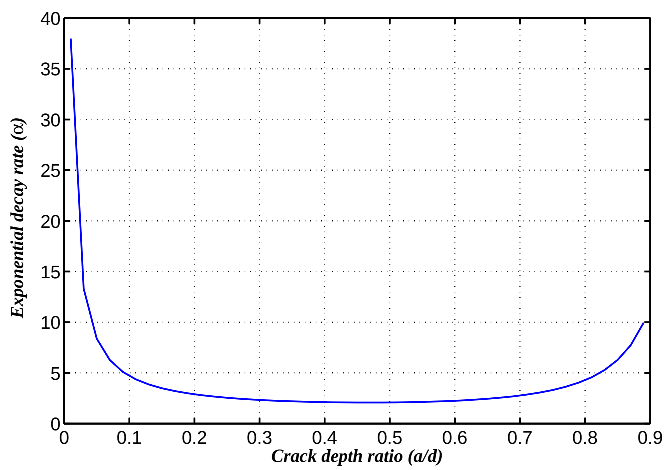

FIG. 3. Exponential decay rate α versus crack depth ratio (a/d) for a crack at the midspan $(x_c/l = 0.5)$.

5. Eigensolution

In order to find the natural frequencies and mode shapes of a cracked beam, the equation of motion presented in Eq. (3.14) must be solved. However, this equation cannot be solved analytically and a numerical method must be used. It can be assumed that the solution is a harmonic function, so one has

$$w(x,t) = X(x)e^{i\omega t}, \tag{5.1}$$

where ω is the natural frequency of the beam. Substituting Eq. (5.1) into Eq. (3.14) and assuming EI_η to be constant along the beam, the following eigenvalue problem is a result:

$$\frac{d^2}{dx^2}\biggl((X''+k_7X''(x_c)e^{-\alpha|x-x_c|/d}) + \frac{\rho}{\kappa G}\omega^2(X+k_7X(x_c)e^{-\alpha|x-x_c|/d})\biggr) - \frac{\rho A}{EI_\eta}\omega^2 X = -\frac{\rho}{E}\omega^2\biggl((X''+k_8X''(x_c)e^{-\alpha|x-x_c|/d}) + \frac{\rho}{\kappa G}\omega^2(X+k_8X(x_c)e^{-\alpha|x-x_c|/d})\biggr). \tag{5.2}$$

Equation (5.2) has a special form, contains a singular function and depends on the value of the solution at the crack position. Theses anomalies prevent one to use the ordinary Galerkin projection method and the normal weighted residual solution for this Sturm–Liouville problem. Behzad *et al.* [21] presented a modified Galerkin projection algorithm for solving this type of equations. In this paper a similar approach has been used. In a regular Sturm–Liouville problem one can easily consider the function X to be in the form of $\sum c_i S_i(x)$ in which $S_i(x)$ are the shape functions that satisfy the physical boundary conditions. However, in this research, the results show that such an approach will lead to divergence of the results. Since the function $e^{-\alpha|x-x_c|/d}$ in Eq. (5.2) is not a smooth function it seems that the solution, especially, for larger crack depth ratios tends to have large derivatives near the crack tip. Accordingly, extracting the value of $X''(x_c)$ from X by derivation can lead to large fluctuations in the results and divergence. In order to avoid the divergence problem, the function X'' and the value of $X''(x_c)$ are not extracted from X by direct derivation. Instead X'' is discretized independently from X and then a constraint equation is provided to link X'' to X.

Considering the above, the following relations can be written:

$$\begin{cases} X''+k_7X''(x_c)e^{-\alpha|x-x_c|/d} = \displaystyle\sum_{i=1}^{N} d_{1i}S_i(x), \\ X+k_7X(x_c)e^{-\alpha\frac{|x-x_c|}{d}} = \displaystyle\sum_{i=1}^{N} d_{2i}S_i(x), \\ X''+k_8X''(x_c)e^{-\alpha|x-x_c|/d} = \displaystyle\sum_{i=1}^{N} d_{3i}S_i(x), \\ X+k_8X(x_c)e^{-\alpha|x-x_c|/d} = \displaystyle\sum_{i=1}^{N} d_{4i}S_i(x), \\ X = \displaystyle\sum_{i=1}^{N} c_iS_i(x), \end{cases} \tag{5.3}$$

in which c_i and d_{1-4i} are independent sets of constants and functions $S_i(x)$ are the shape functions which must satisfy the physical boundary conditions.

Substituting Eq. (5.3) into Eq. (5.2), multiplying two sides of the equation by $S_j(x)$, and then integrating along the length of the beam, one has

$$\begin{aligned}(5.4)\qquad &\sum_{i=1}^{N} d_{1i}\int_0^l S_i''(x)S_j(x)dx\\ &+\frac{\rho}{\kappa G}\omega^2\sum_{i=1}^{N} d_{2i}\int_0^l S_i''(x)S_j(x)dx-\frac{\rho A}{EI_\eta}\omega^2\sum_{i=1}^{N} c_i\int_0^l S_i(x)S_j(x)dx\\ &+\frac{\rho}{E}\omega^2\left(\sum_{i=1}^{N} d_{3i}\int_0^l S_i''(x)S_j(x)dx+\frac{\rho}{\kappa G}\omega^2\sum_{i=1}^{N} d_{4i}\int_0^l S_i''(x)S_j(x)dx\right)=0,\end{aligned}$$

$j = 1, 2, \ldots, N$. Or in the matrix form:

$$\begin{aligned}(5.5)\qquad &\mathbf{K}_1\mathbf{d}_1+\omega^2\left(\mathbf{M}_1\mathbf{d}_2+\mathbf{M}_2\mathbf{c}+\mathbf{M}_3\mathbf{d}_3\right)+\omega^4\mathbf{D}_1\mathbf{d}_4=0,\\ &K_{1ij}=\int_0^l S_i''(x)S_j(x)dx, \qquad M_{1ij}=\frac{\rho}{\kappa G}\int_0^l S_i''(x)S_j(x)dx,\\ &M_{2ij}=-\frac{\rho A}{EI_\eta}\int_0^l S_i(x)S_j(x)dx, \qquad M_{3ij}=\frac{\rho}{E}\int_0^l S_i(x)S_j(x)dx,\\ &D_{1ij}=\frac{\rho^2}{\kappa GE}\int_0^l S_i(x)S_j(x)dx.\end{aligned}$$

On the other hand, the following relations can be obtained from (5.5):

$$(5.6)\qquad \begin{cases}\displaystyle\sum_{i=1}^{N} d_{1i}S_i''(x)=\frac{1}{1+k_7}\sum_{i=1}^{N} c_iS_i(x),\\ \displaystyle\sum_{i=1}^{N} d_{2i}S_i(x)=\frac{1}{1+k_7}\sum_{i=1}^{N} c_iS_i(x),\\ \displaystyle\sum_{i=1}^{N} d_{3i}S_i''(x)=\frac{1}{1+k_8}\sum_{i=1}^{N} c_iS_i(x),\\ \displaystyle\sum_{i=1}^{N} d_{4i}S_i(x)=\frac{1}{1+k_8}\sum_{i=1}^{N} c_iS_i(x).\end{cases}$$

Multiplying two sides of Eq. (5.6) by $S_j(x)$, integrating along the length of the beam and writing the equations in the matrix form, one has:

$$
\begin{gathered}
\mathbf{d}_1=\mathbf{P}_1^{-1}\mathbf{Q}_1\mathbf{c}, \qquad \mathbf{d}_2=\mathbf{P}_1^{-1}\mathbf{Q}_2\mathbf{c},\\
\mathbf{d}_3=\mathbf{P}_2^{-1}\mathbf{Q}_1\mathbf{c}, \qquad \mathbf{d}_4=\mathbf{P}_2^{-1}\mathbf{Q}_2\mathbf{c},\\
Q_{1ij}=\int_0^l S_i''(x)S_j(x)\,dx, \qquad Q_{2ij}=\int_0^l S_i(x)S_j(x)\,dx,\\
P_{1ij}=\int_0^l S_i(x)S_j(x)\,dx-\frac{k_7}{1+k_7}\int_0^l S_i(x)S_j(x)\,dx,\\
P_{2ij}=\int_0^l S_i(x)S_j(x)\,dx-\frac{k_8}{1+k_8}\int_0^l S_i(x)S_j(x)\,dx.
\end{gathered}
\tag{5.7}
$$

Substituting Eq. (5.7) into Eq. (5.5), the following equation is obtained:

$$
\begin{aligned}
&(\mathbf{K}+\omega^2\mathbf{M}+\omega^4\mathbf{D})\mathbf{c}=\mathbf{0}, && \mathbf{K}=\mathbf{K}_1\mathbf{P}_1^{-1}\mathbf{Q}_1,\\
&\mathbf{M}=\mathbf{M}_1\mathbf{P}_1^{-1}\mathbf{Q}_2+\mathbf{M}_2+\mathbf{M}_3\mathbf{P}_2^{-1}\mathbf{Q}_1, && \mathbf{D}=\mathbf{D}_1\mathbf{P}_2^{-1}\mathbf{Q}_2.
\end{aligned}
\tag{5.8}
$$

The natural frequencies and corresponding mode shapes for the cracked beam can be calculated by solving the matrix eigenvalue problem of Eq. (5.8).

6. Results for a simply supported beam with rectangular cross-section

In this section, the beam is assumed to be simply supported with a rectangular cross-section. However, for every desired boundary condition and cross-section, the presented solution can be used. The beam is modeled with an aspect ratio of 5 and properties described in Table 1.

Table 1. Properties used for modeling the cracked beam.

Property	Value
Dimensions $L\times d\times b(m)$	$1.25e-1\times 2.5e-2\times 5e-3$
Modulus of elasticity E (GPa)	200
Shear modulus G (GPa)	76.9
Poisson's ratio ν	0.3
Density ρ (kg/m^3)	7810
Timoshenko shear coefficient κ	5/6

In a simply supported cracked beam the shape functions $S_i(x)$ can be assumed to be in the form of $\sin(i\pi x/l)$ which satisfies the physical boundary conditions. In this research, the number of shape functions N is set to be 100. The natural frequencies and mode shapes have been calculated using Eq. (5.8).

Figure 4 shows the first three natural frequency ratios of the Timoshenko cracked beam. In order to generalize the results, the natural frequencies of the cracked beam have been divided to the corresponding values for a normal beam. In Fig. 4, the natural frequency ratios have been plotted versus the crack depth ratio (a/d) for several crack positions, $x_c/l = 0.1$, 0.3 and 0.5.

To verify the results, they are compared with results of the finite element (FE) analysis in Fig. 4. ANSYS software has been used for the finite element analysis. In order to have an accurate and reliable model, the PLANE183 singular element has been used in the cracked area [25]. This element is an eight-node quadratic solid singular element which is specially designed for the crack analysis. In this research, a fine mesh has been used at the vicinity of the crack and dependency of the results on the mesh size has been checked. In all of the results there is a good agreement between analytical results and FE analysis results.

The first three natural frequencies obtained by the proposed model are compared to Carneiro and Inman's [19] analytical and finite element results for a crack at $x_c/l = 0.5$ in Fig. 5. In this figure, results are divided by corresponding natural frequencies of an uncracked beam. They show a good agreement that verifies the accuracy of the proposed model.

The first three natural frequencies of Euler–Bernoulli [21] and Timoshenko cracked beams are compared with each other in Fig. 6. In this figure, the results of natural frequencies are divided by corresponding natural frequencies of uncracked Timoshenko beam. In the case of healthy beam, the Euler–Bernoulli beam has 6, 22 and 42 percent difference in comparison to Timoshenko beam for the first three natural frequencies, respectively, as it can be seen in Fig. 6. This shows the importance of using Timoshenko beam model in the case of short beams. Also, the Euler–Bernoulli beam has higher sensitivity to the crack depth rather than Timoshenko beam.

Figure 7 shows the first three normalized mode shapes for a cracked beam with $a/d = 0.5$ and $x_c/l = 0.1$, 0.3 and 0.5. Comparison of the analytical and finite element results in this figure shows the efficiency of the presented model in modeling of mode shapes.

Effect of crack position ratio (x_c/l) on the first and second mode shapes is shown in Figs. 8 and 9, respectively, for $a/d = 0.1$, 0.3 and 0.5.

Figures 10 and 11 show effect of crack depth ratio (a/d) on the first and second mode, respectively, for $x_c/l = 0.1$, 0.3 and 0.5.

Results show that the decrease in natural frequencies and the change in mode shapes are dependent on both crack depth ratio and crack position. In general, a higher crack depth ratio leads to a bigger change in natural frequencies and mode shapes for a given crack position. But in the case of crack position, the

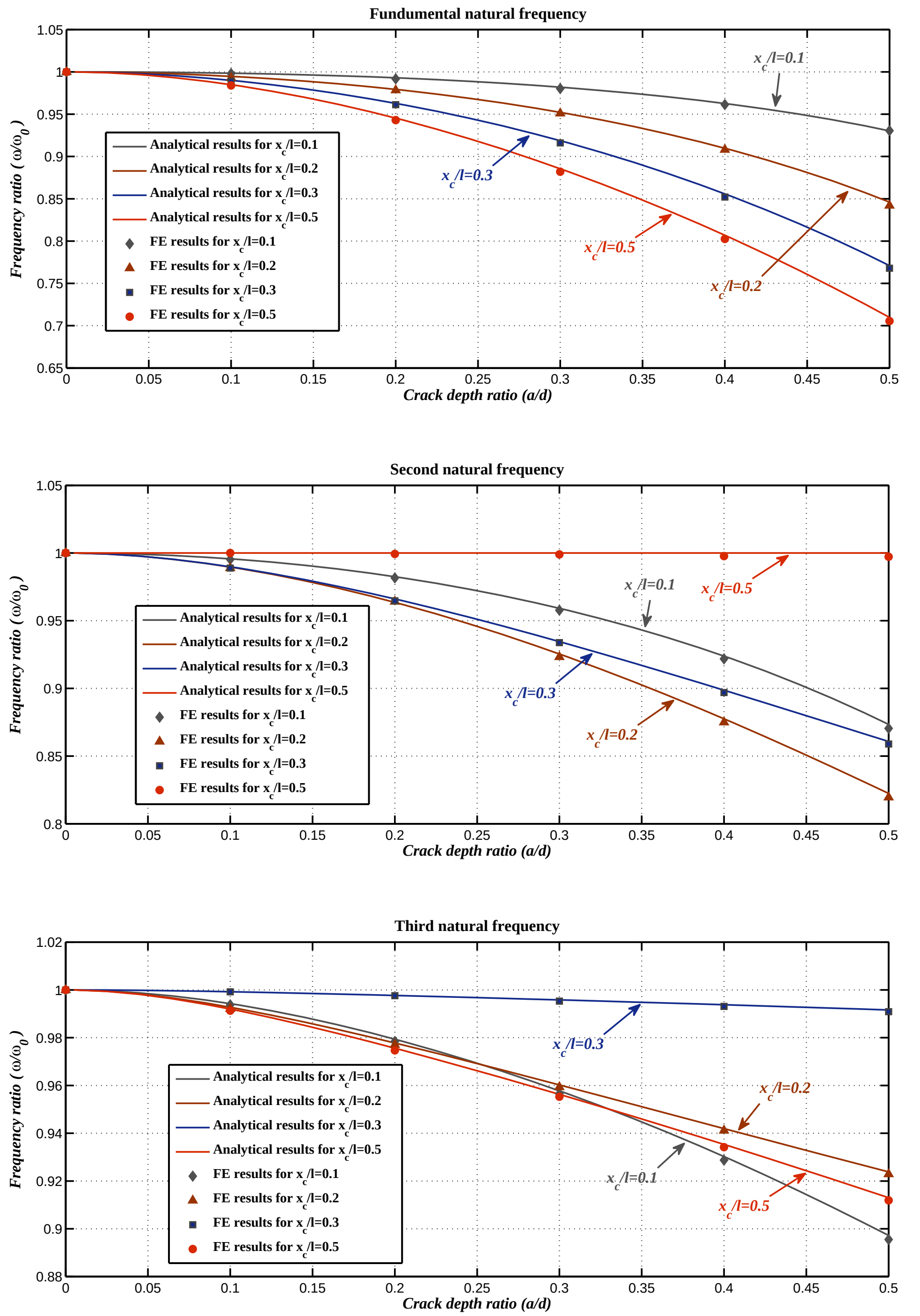

Fig. 4. First three natural frequency ratios of a cracked beam versus crack depth ratio (a/d).

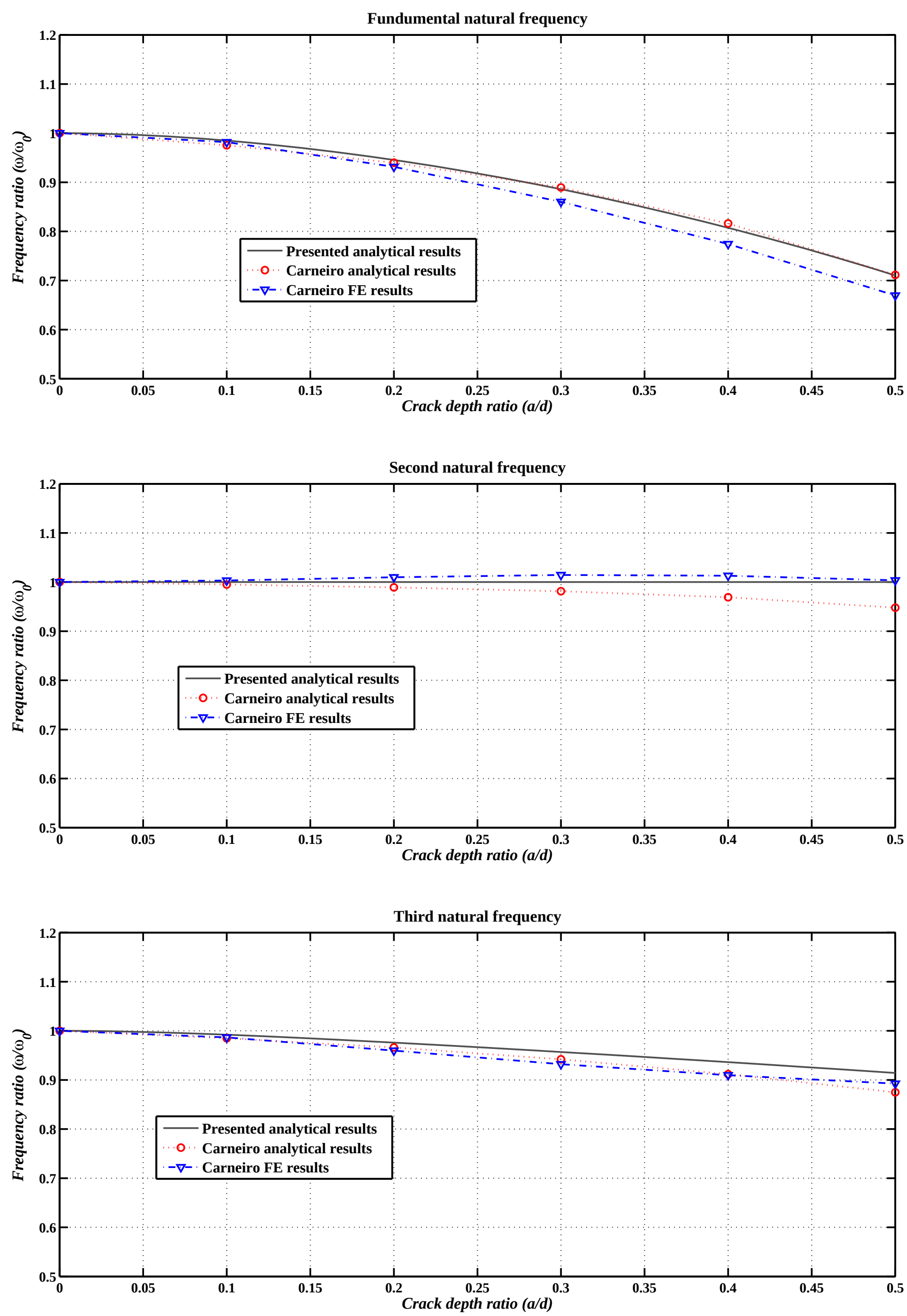

FIG. 5. First three natural frequency ratios of a cracked beam versus crack depth ratio (a/d) for crack position ratio $x_c/l = 0.5$; comparison with CARNEIRO and INMAN'S [19] analytical and finite element results and the present work.

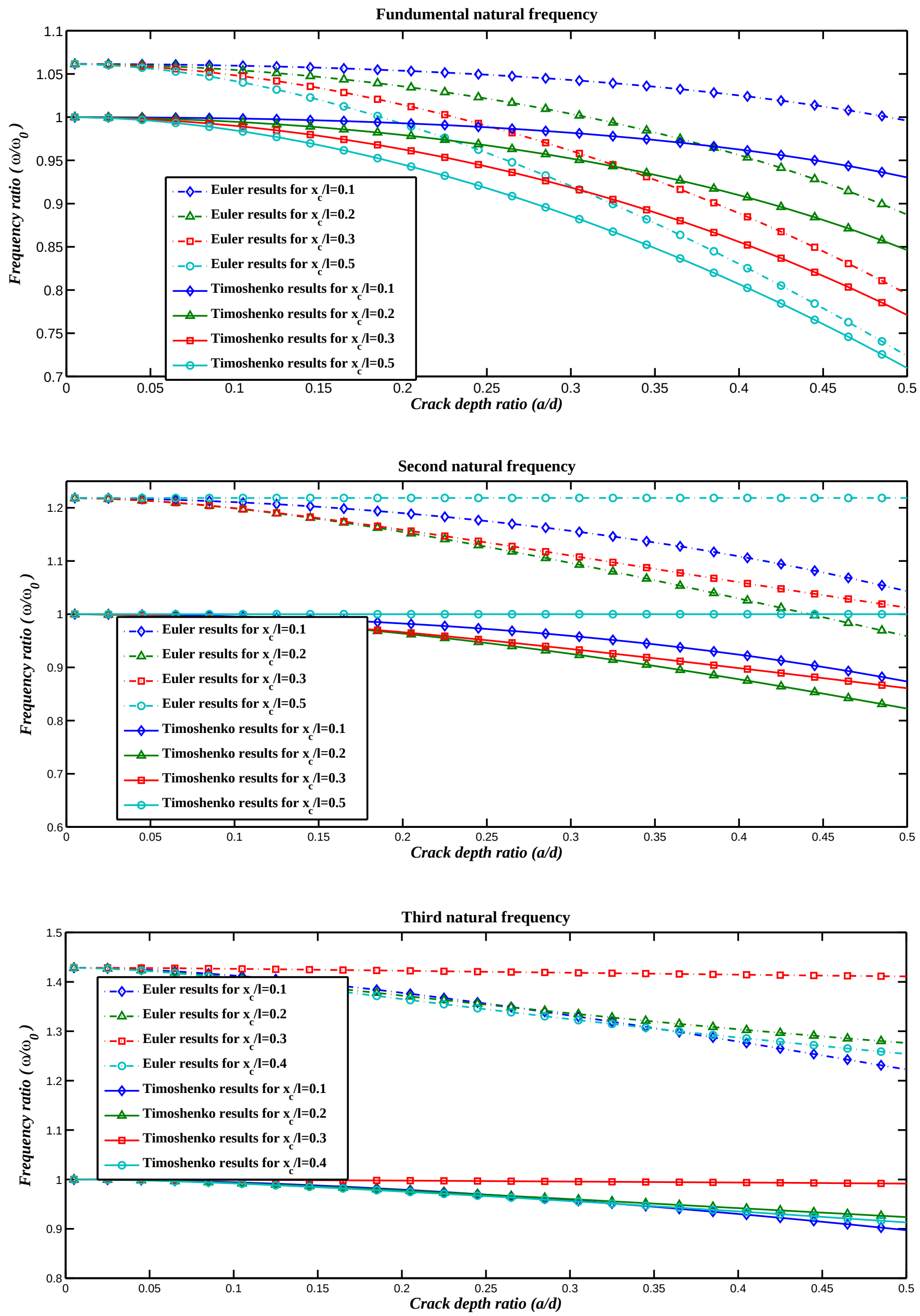

Fig. 6. First three natural frequency ratios of a cracked beam versus crack depth ratio (a/d); comparison with Timoshenko and Euler–Bernoulli [21] cracked beam models.

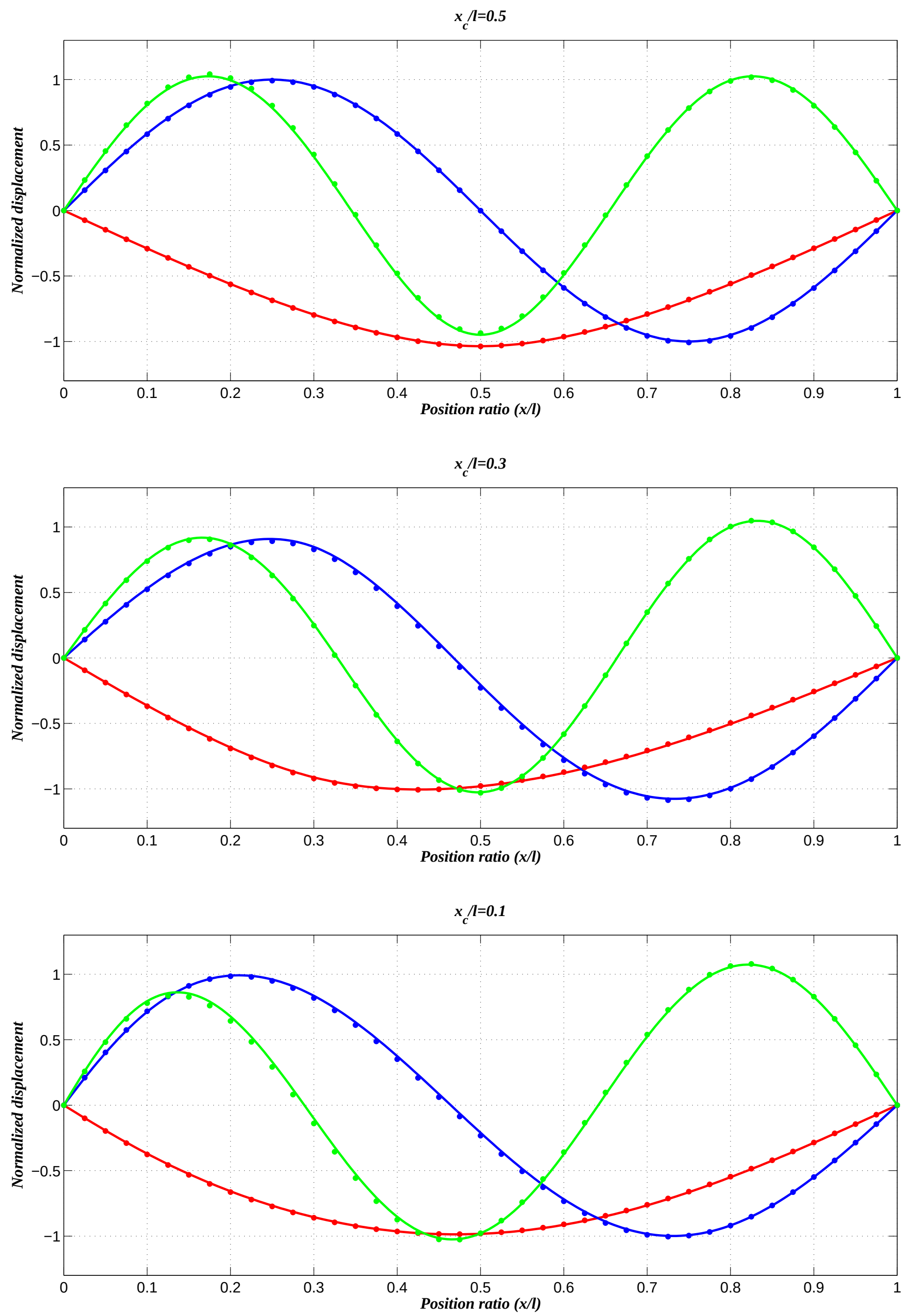

FIG. 7. First three normalized mode shapes of a cracked beam with $a/d = 0.5$; (——): analytical results; (●●●●): finite element results.

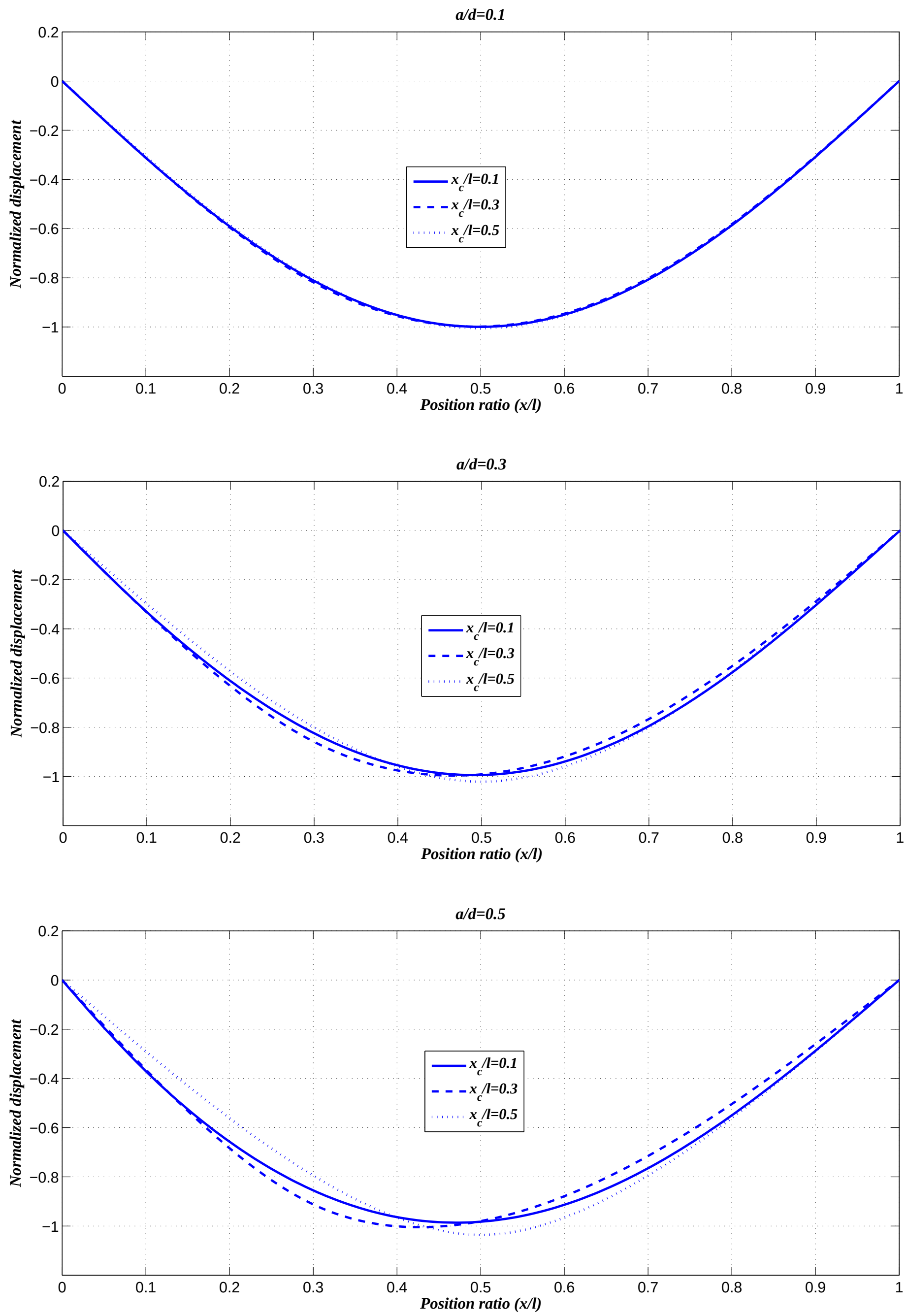

Fig. 8. Effect of crack position ratio (x_c/l) on first normalized mode shape of a cracked beam.

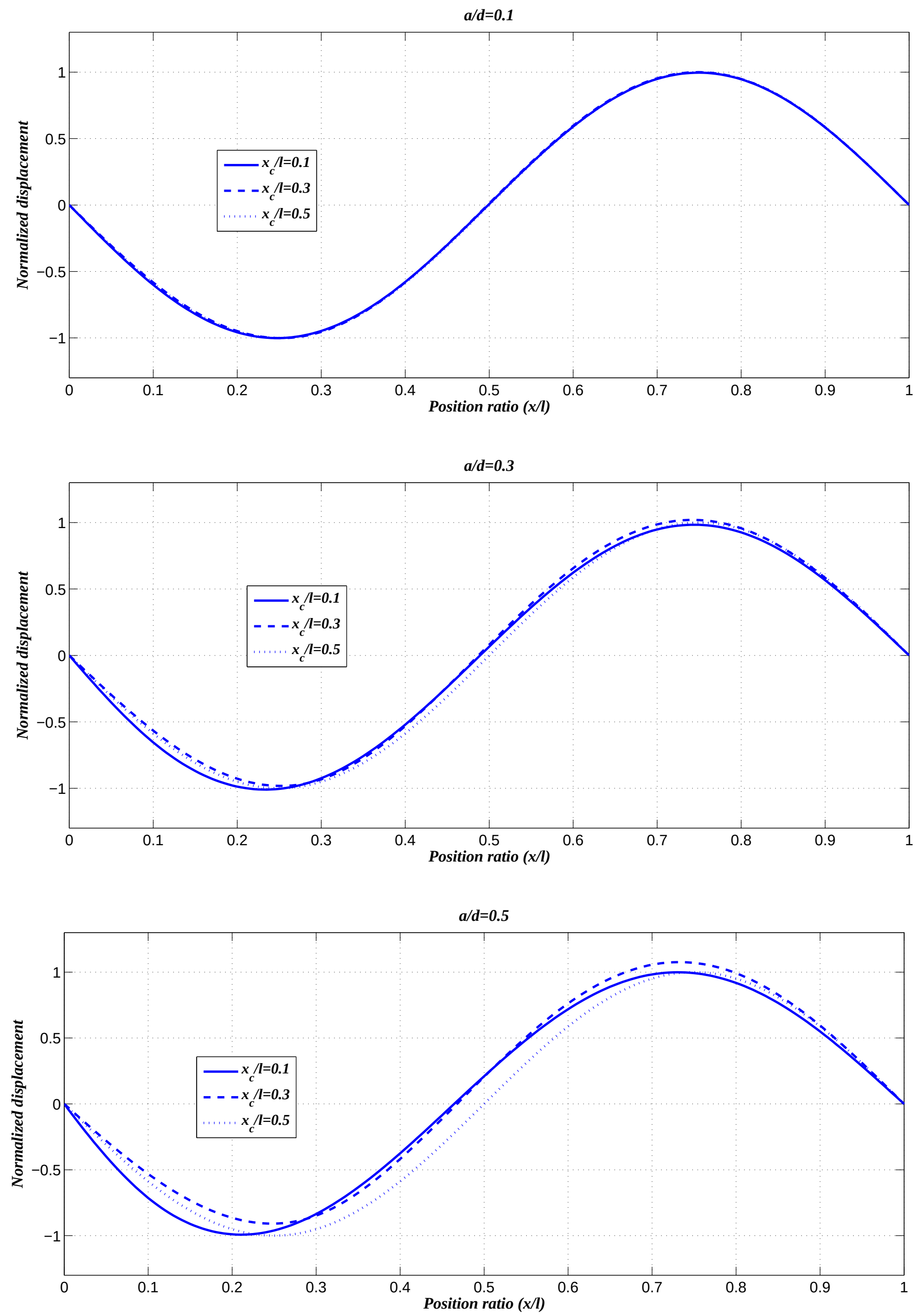

FIG. 9. Effect of crack position ratio (x_c/l) on second normalized mode shape of a cracked beam.

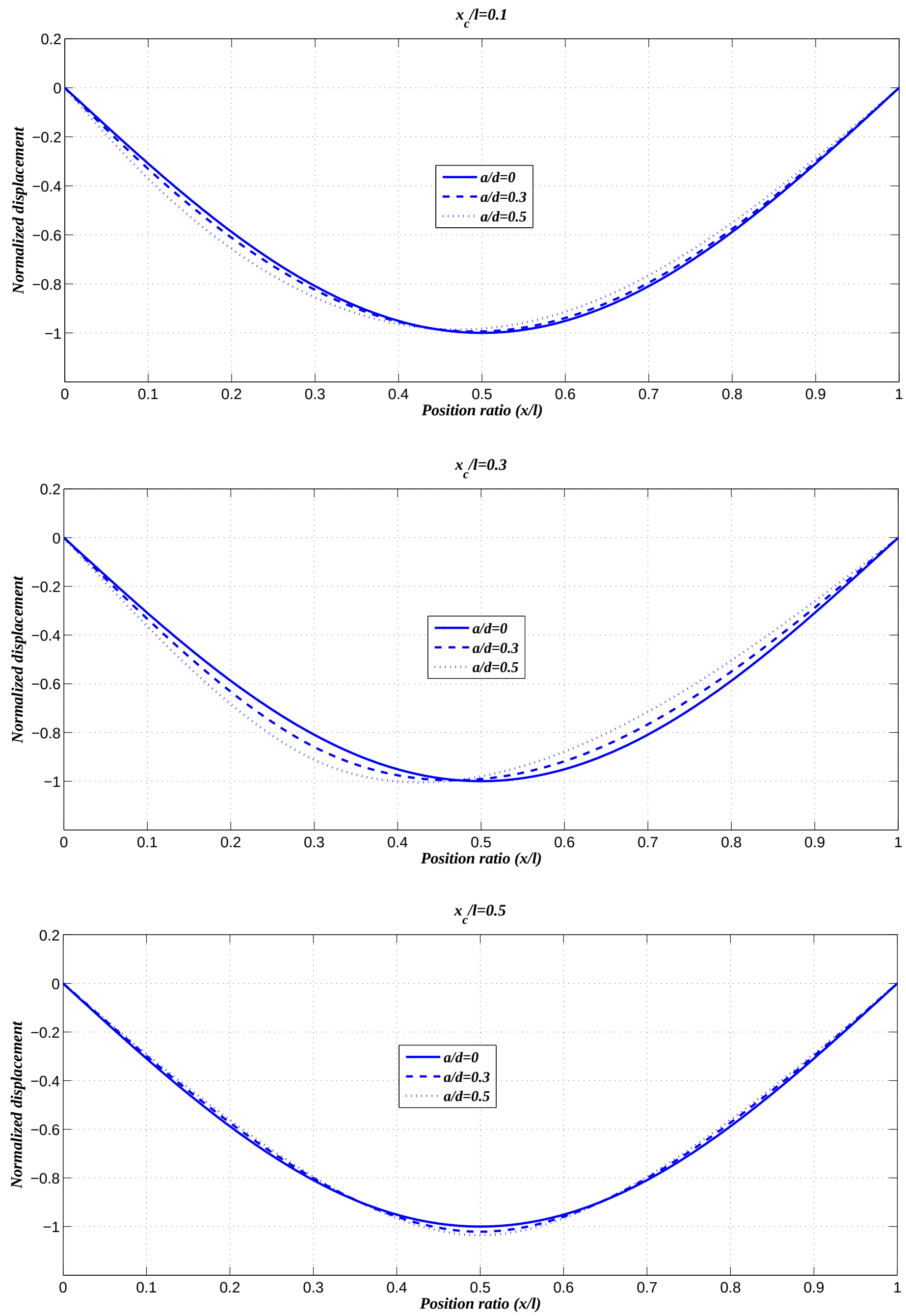

Fig. 10. Effect of crack depth ratio (a/d) on first normalized mode shape of a cracked beam.

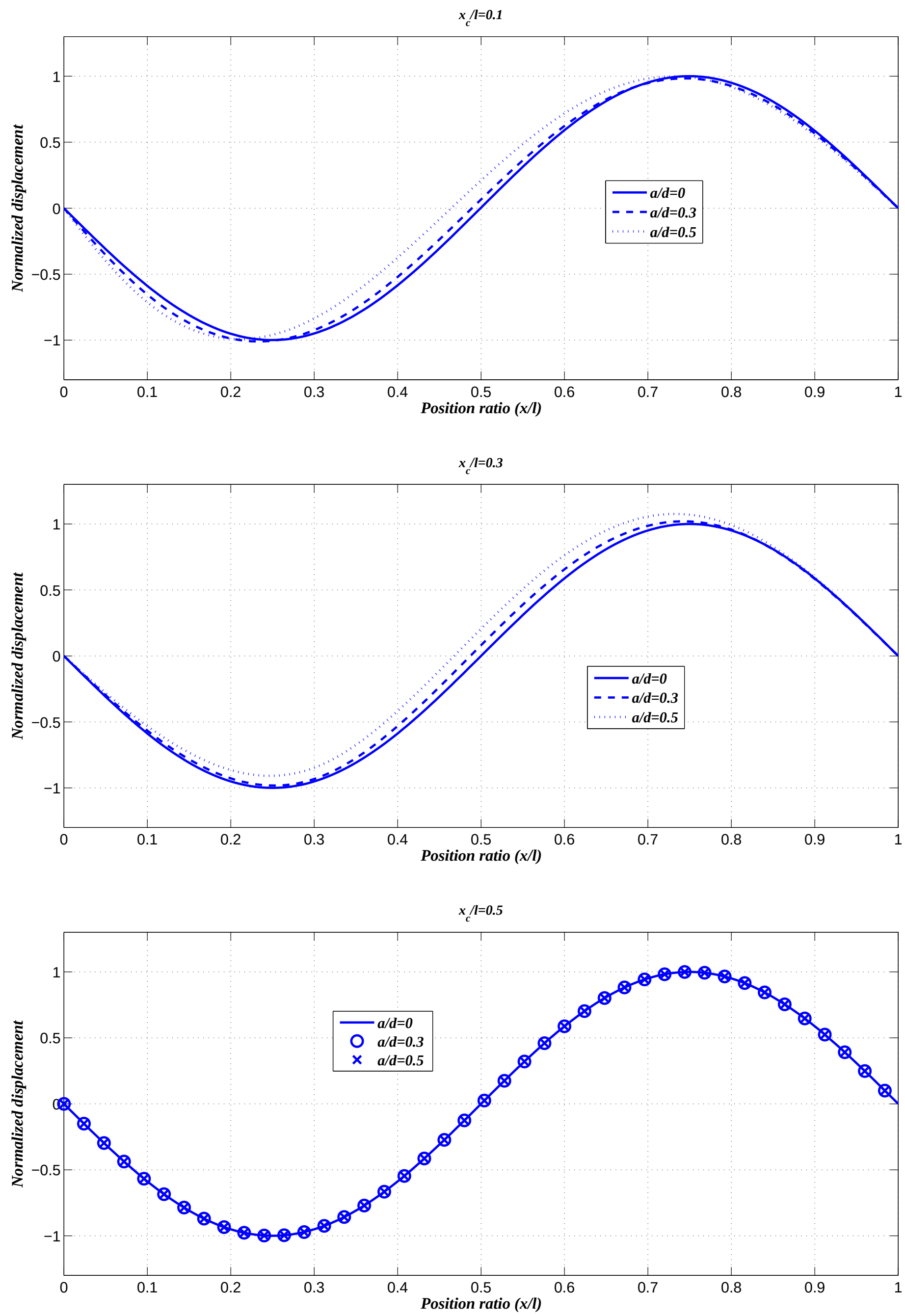

FIG. 11. Effect of crack depth ratio (a/d) on second normalized mode shape of a cracked beam.

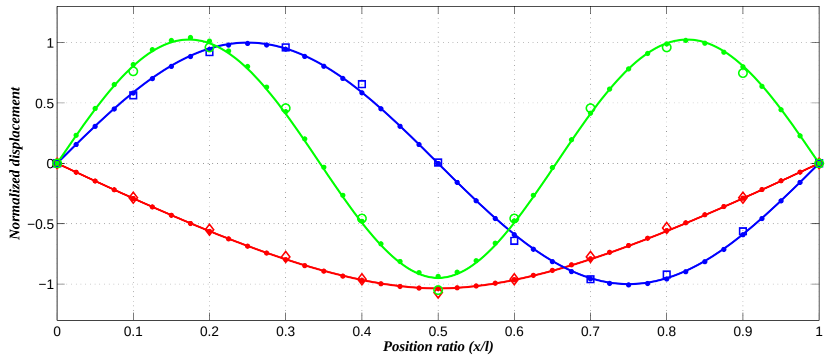

Fig. 12. Comparison of the first three normalized mode shapes with Carneiro and Inman's [19] analytical results and the analytical and finite element results for a cracked beam with $a/d = 0.5$ and $x_c/l = 0.5$. (——): analytical results; (●●●●): finite element results; (◇◇◇◇), (□□□□), (○○○○): Carneiro and Inman's analytical results.

amount of change is dependent on the position of crack relative to the nodes and anti-nodes of the corresponding mode shape. For a crack at the node of mode shape, there is no change in the natural frequencies and mode shapes, but for a crack at the anti-node of mode shapes, the change has its maximum amount. As it can be observed in Figs. 4 and 11, the second natural frequency and mode shape do not show any change for a crack at the midspan of the beam ($x_c/l = 0.5$) because this point coincides with the node of the second mode of the beam. But as it can be seen in Figs. 4 and 10, the first natural frequency and mode shape show their maximum change for a crack at the midspan. This is becausethe midspan is the anti-node of the first mode shape. The first three mode shapes of a cracked beam are compared with Carneiro and Inman's analytical results [19] and the proposed analytical and finite element results for a crack at $x_c/l = 0.5$ and $a/d = 0.5$ in Fig. 12. This comparison shows higher accuracy of the proposed model in determining mode shapes of a cracked beam in comparison to Carneiro and Inman's results [19].

7. Conclusions

A continuous theory for the flexural vibration analysis of a Timoshenko beam with an open edge crack has been developed in this paper. A bilinear displacement field [21] has been suggested for the beam. In the proposed displacement field, it is assumed that the crack face rotates more than the other parts of the section as well as its adjacent area. Also, the additional rotation decays with an exponential regime along the beam length. The strain and stress fields are calculated by direct derivation of displacement field and using the linear elastic material model. Next, the partial differential equation of motion has been obtained using Hamilton's principle with considering the effects of shear strain and rotary inertia.

The obtained governing equation of motion for a simply supported beam with a rectangular cross-section and an open edge crack has been solved with a modified Galerkin projection method. The obtained results have been compared with finite element results for the first three natural frequencies and mode shapes and an excellent agreement has been observed. Also, a good agreement has been observed between presented results and previous work results [19] for the first three natural frequencies. Furthermore, a higher accuracy in the results of first three mode shapes has been observed compared to the previous model [19].

Results for the first three natural frequencies have also been compared with Euler–Bernoulli beam [21] to show the importance of using Timoshenko model in the case of short beams. The obtained results have also been used to study the effect of crack parameters on natural frequencies and mode shapes. Results show that the change in the natural frequencies and mode shapes is dependent on both crack depth ratio and crack position.

The presented model proposes a reasonably accurate model which predicts the behavior of a cracked short beam and its results are reliable near the crack tip and far from it. Additionally, the displacement and strain fields are completely compatible in this model, while in the previous continuous models, an inconsistency existed between strain and displacement fields which can cause inaccuracy in results. The developed theory is applicable for open edge cracks and there is a need for an extension to breathing cracks and other types of cracks.

References

1. A.D. Dimarogonas, *Vibration of cracked structures: a state of the art review*, Engineering Fracture Mechanics, **5**, 831–857, 1996.
2. J. Wauer, *On the dynamics of cracked rotors: a literature survey,* Applied Mechanics Reviews, **43**, 1, 13–17, 1990.
3. R. Gasch, *A survey of the dynamic behavior of a simple rotating shaft with a transverse crack*, Journal of Sound and Vibration, **160**, 2, 313–332, 1993.
4. A.D. Dimarogonas, S.A. Paipetis, *Analytical methods in rotor dynamics*, Applied Science Publisher, London, 1983.
5. D.Y. Zheng, S.C. Fan, *Vibration and stability of cracked hollow-sectional beams*, Journal of Sound and Vibration, **267**, 933–954, 2003.
6. J. Yang, Y. Chen, Y. Xiang, X.L. Jia, *Free and forced vibration of cracked inhomogeneous beams under an axial force and a moving load*, Journal of Sound and Vibration, **312,** 166–181, 2008.
7. H.P. Lin, *Direct and inverse methods on free vibration analysis of simply supported beams with a crack*, Engineering Structures, **26**, 4, 427–436, 2004.

8. D.Y. Zheng, S.C. Fan, *Vibration and stability of cracked hollow-sectional beams*, Journal of Sound and Vibration, **267**, 933–954, 2003.
9. J.A. Loya, L. Rubio, J. Fernandez-Saez, *Natural frequencies for bending vibrations of Timoshenko cracked beams*, Journal of Sound and Vibration, **290**, 640–653, 2006.
10. S. Orhan, *Analysis of free and forced vibration of a cracked cantilever beam*, NDT&E International, **40**, 443–450, 2007.
11. X.F. Yang, A.S.J. Swamidas, R. Seshadri, *Crack identification in vibrating beams using the energy method*, Journal of Sound and Vibration, **244**, 2, 339–357, 2001.
12. J. Wang, P. Qiao, *Vibration of beams with arbitrary discontinuities and boundary conditions*, Journal of Sound and Vibration, **308**, 12–27, 2007.
13. S. Christades, A.D.S. Bar, *One-dimensional theory of cracked Bernoulli-Euler beams*, Journal of Mechanical Science, **26**, 639–648, 1984.
14. M.H.H. Shen, C. Pierre, *Natural modes of Bernoulli-Euler beams with symmetric cracks*, Journal of Sound and Vibration, **138**, 1, 115–134, 1990.
15. M.H.H. Shen, C. Pierre, *Free vibrations of beams with a single-edge crack*, Journal of Sound and Vibration, **170**, 2, 237–259, 1994.
16. S.H.S. Carneiro, D.J. Iinman, *Comments on the free vibration of beams with a single-edge crack*, Journal of Sound and Vibration, **244**, 4, 729–737, 2001.
17. T.G. Chondros, A. D. Dimarogonas, J. Yao, *A continuous cracked beam vibration theory*, Journal of Sound and Vibration, **215**, 1, 17–34, 1998.
18. T.G. Chondros, A.D. Dimarogonas, J. Yao, *Vibration of a beam with breathing crack*, Journal of Sound and Vibration, **239**, 1, 57–67, 2001.
19. S.H.S. Carneiro, D.J. Inman, *Continuous model for the transverse vibration of cracked Timoshenko beams*, Journal of Vibration and Acoustics, **124**, 310–320, 2002.
20. M. Behzad, A. Meghdari, A. Ebrahimi, *A linear theory for bending stress–strain analysis of a beam with an edge crack*, Engineering Fracture Mechanics, **75**, 16, 4695–4705, 2008.
21. M. Behzad, A. Meghdari, A. Ebrahimi, *A new continuous model for flexural vibration analysis of a cracked beam*, Polish Maritime Research, **15**, 2, 32–39, 2008.
22. M. Behzad, A. Meghdari, A. Ebrahimi, *A new approach for vibration analysis of a cracked beam*, International Journal of Engineering, **18**, 4, 319–330, 2005.
23. M. Behzad, A. Meghdari, A. Ebrahimi, *A continuous model for forced vibration analysis of a cracked beam*, ASME International Mechanical Engineering Congress and Exposition, IMECE 2005, Orlando, Florida, 2005.
24. M. Behzad, A. Ebrahimi, A. Meghdari, *A continuous vibration theory for beams with a vertical edge crack*, Scientica Iranica Transaction B: Mechanical Engineering, **17**, 3, 194–204, 2010.
25. ANSYS User's Manual for rev. 8, ANSYS Inc., 2004.

Received October 23, 2012; revised version April 13, 2013.